










Article

In Situ X-ray Absorption Spectroscopy Cells for High Pressure Homogeneous Catalysis

Petr V. Shvets ^{1,*}, Pavel A. Prokopovich ¹, Artur I. Dolgoborodov ¹, Oleg A. Usoltsev ², Alina A. Skorynina ², Elizaveta G. Kozyr ^{2,3}, Viktor V. Shapovalov ², Alexander A. Guda ², Aram L. Bugaev ², Evgeny R. Naranov ⁴, Dmitry N. Gorbunov ⁴, Kwinten Janssens ⁵, Dirk E. De Vos ⁵, Alexander L. Trigub ⁶, Emiliano Fonda ⁷, Mark B. Leshchinsky ⁸, Vladimir R. Zagackij ⁹, Alexander V. Soldatov ² and Alexander Yu. Goikhman ¹

¹ Research and Educational Center “Functional Nanomaterials”, I. Kant Baltic Federal University, A. Nevskogo 14, Kaliningrad 236041, Russia

² The Smart Materials Research Institute, Southern Federal University, Sladkova 178/24, Rostov-on-Don 344090, Russia

³ Department of Chemistry, University of Turin, Via Giuria 5, 10125 Torino, Italy

⁴ Topchiev Institute of Petrochemical Synthesis, Russian Academy of Sciences, Leninskiy Prospekt 29, Moscow 119991, Russia

⁵ Centre for Membrane Separations, Adsorption, Catalysis and Spectroscopy for Sustainable Solutions (cMACS), KU Leuven, Celestijnenlaan 200F, 3001 Leuven, Belgium

⁶ National Research Centre “Kurchatov Institute”, Ak. Kurchatov Sq. 1, Moscow 123182, Russia

⁷ Synchrotron SOLEIL, L’Orme des Merisiers, Saint-Aubin, 91192 Gif-sur-Yvette, France

⁸ Chair of Automated Machine Engineering, Kaliningrad State Technical University, Sovietsky Prospekt 1, Kaliningrad 236022, Russia

⁹ Department of Shipbuilding and Energetics, Kaliningrad State Technical University, Sovietsky Prospekt 1, Kaliningrad 236022, Russia

* Correspondence: pshvets@kantiana.ru



Citation: Shvets, P.V.; Prokopovich, P.A.; Dolgoborodov, A.I.; Usoltsev, O.A.; Skorynina, A.A.; Kozyr, E.G.; Shapovalov, V.V.; Guda, A.A.; Bugaev, A.L.; Naranov, E.R.; et al. In Situ X-ray Absorption Spectroscopy Cells for High Pressure Homogeneous Catalysis. *Catalysts* **2022**, *12*, 1264. <https://doi.org/10.3390/catal12101264>

Academic Editor: Maria Luisa Di Gioia

Received: 16 September 2022

Accepted: 13 October 2022

Published: 17 October 2022

Publisher’s Note: MDPI stays neutral with regard to jurisdictional claims in published maps and institutional affiliations.



Copyright: © 2022 by the authors. Licensee MDPI, Basel, Switzerland. This article is an open access article distributed under the terms and conditions of the Creative Commons Attribution (CC BY) license (<https://creativecommons.org/licenses/by/4.0/>).

Abstract: We have designed, built, and tested two cells for in situ and, potentially, operando X-ray absorption spectroscopy experiments in transmission and fluorescence modes. The cells were developed for high-pressure and high-temperature conditions to study the catalytic processes under relevant industrial conditions. Operation of the cells was tested for Ru and Rh-based homogeneous and heterogeneous catalytic systems. Using synchrotron-based in situ X-ray absorption spectroscopy we tracked the evolution of active metal species during catalytic reactions. Our setup proved that it was capable to investigate liquid-state homogeneous and heterogeneous systems under elevated temperatures, high pressures of reactive gasses, and in the presence of corrosive reagents.

Keywords: operando cell; X-ray absorption spectroscopy; XANES; in situ measurements; homogeneous catalysis; heterogeneous catalysis; high-pressure cell; Ru-based catalysts; Rh-based catalysts

1. Introduction

Operando spectroscopy allows for the real-time monitoring of the structural evolution, activity, and selectivity of catalytic systems [1,2]. Currently, operando methodology is aimed at narrowing the gap between conditions used in industry and those achievable in research reactors (high pressures and temperatures, differences between model and real catalysts) [3]. Liquid-phase reactions and reactions in the presence of homogeneous catalysts are an important part of industrial processes, but operando experiments for such systems are still challenging [4].

Investigations using hard X-rays generated by synchrotrons make it possible to study processes both on the surface and in the volume of catalysts with high time resolution [5]. Since X-ray absorption spectroscopy (XAS) is selective toward chemical elements, it is an effective tool to monitor local atomic and electronic structures around active metal centers

in operando mode [6]. However, such experiments are commonly limited to heterogeneous catalysts where a catalyst is present in the form of a pellet or powder and chemical reactions in a gaseous phase [7–9]. Reactions in a liquid phase are diverse and have important practical applications, but there are only a few reports investigating such systems using synchrotron radiation [10,11]. Much fewer reports can be found in the field of homogeneous catalysis due to the complexity of the research setups.

In situ and operando investigations require special cells, which sustain controllable conditions around the sample. Such cells are designed to keep vacuum or high pressure [12–14], low or high temperatures [15–17], and a special gaseous or liquid environment [18,19] inside the closed volume. Some cells are specially produced to investigate the electrochemical performance of battery materials [20,21] and catalytic processes [22–24].

Despite the large number of research works devoted to the development of special cells, it is still a crucial task to construct cells combining different conditions simultaneously, for instance, high temperature and high pressure, for specific applications. Such cells must be equipped with certain windows for the implementation of common X-ray investigation methods [25], such as XAS, X-ray diffraction, small-angle X-ray scattering, etc. Optical ports for infrared (IR) or ultraviolet radiation might be necessary as well along with a set of sensors inside a cell to control and maintain required inner conditions.

The majority of the cells mentioned above allow for the realization of one research method and variation of one environmental parameter. Developing and building cells, which can utilize different investigation techniques under a set of different conditions is a greater challenge. Special flow cells, which are used to monitor chemical reactions in situ, involve additional technical requirements (use of pipeline valves and pumping system). Nevertheless, overcoming these challenges is worthwhile, because such cells can offer insights into the catalyst activation processes, phase behavior, kinetics, and mechanisms of catalysis reactions [26–29].

In this work, we present two autoclave-type cells developed to measure X-ray absorption spectra under high-temperature (up to ca. 200 °C) and high-pressure (up to 200 bar) in transmission and fluorescence modes. The cells were tested on homogeneous reactions in a highly absorbing ionic liquid medium and X-ray transparent catalytic system based on Ru and Rh-based homogeneous and heterogeneous catalysts.

2. Results and Discussion

2.1. Cell Design

The developed cells were designed to investigate homogeneous catalytic reactions in the liquid phase in a corrosive environment at the gas-liquid interface. The cells had to sustain temperatures of up to 200 °C and pressures of up to 200 bar, since high pressures enhance the gas concentration in the liquid phase. Such conditions are relevant for various important industrial processes [30]. The first cell, which is referred to below as the fluorescence cell, was designed for highly absorbing media or samples with a low concentration of metal species in the catalytic system that require a fluorescence regime of acquisition. The second cell, the transmission cell, was designed for transmission mode data collection appropriate for the catalyst with sufficient metal loadings in an aqueous or organic solvent medium, transparent for hard X-rays.

The schematic of the fluorescence cell is given in Figure 1a. A cell body (1) was made of steel and has a cylinder cavity. A screwed nozzle was located at one of the sides of the cell and an M24 screw (2) can be attached to it. Three stainless steel tubes were welded to the screw. The tubes were attached to a Swagelok fitting with a screw plug for working mixture inflow (3), a valve for gas outflow (4), and a pressure gauge (5). An X-ray transparent window (6) was made of glassy carbon SIGRADUR® K. The window had a shape of a blunted cone with an apex angle of 90°. Such a shape increases the solid angle for the fluorescence signal from the solution. Polytetrafluoroethylene support rings (7, 8) were placed above and below the window to protect it from cracking at contact with a flange (9) or the cell body. A chemically inert polytetrafluoroethylene reaction box

(10) was mounted inside the cell. The temperature was controlled by four compact 50 W cylindrical heaters (11) and a type K thermocouple (12) attached to the channel in the cell body. The working volume of the cell was 9.08 mL. Figure 1b shows the cell under operating conditions, including the environment and the beam path.

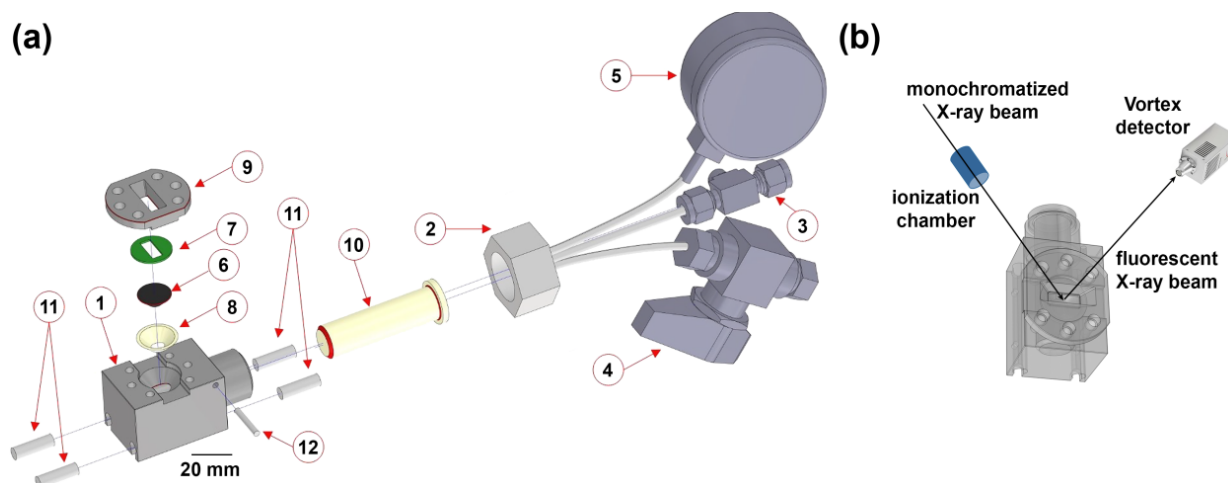


Figure 1. (a) Schematic view of the fluorescence cell. 1—cell body, 2—screw, 3—inlet fitting, 4—outlet valve, 5—pressure gauge, 6—glassy carbon X-ray transparent window, 7, 8—Teflon protecting rings, 9—flange, 10—Teflon reaction vessel, 11—heating elements, 12—thermocouple. (b) Schematic view of the cell under operating conditions.

The transmission cell was designed to perform XAS experiments in the transmission mode improving the spectra obtained at high energies of an incident X-ray beam or for solutions with a low atomic number of the atoms in a solvent (water, organic solvents). The schematic view of the cell is provided in Figure 2. Compared to the fluorescence cell, it does not require a separate X-ray transparent window, which supported the inner Teflon reaction vessel mechanically from distorting at high pressures. Instead of the glassy carbon window, the X-ray beam enters the transmission through a small 2 mm hole (1) in a steel cell body (2) and exits through a similar exit hole placed collinearly. An aluminum tube inset (3) protects a polytetrafluoroethylene reaction box (4) from breaking in high-temperature and high-pressure conditions. Such a design was not suitable for the fluorescence cell because it would require a larger and, consequently, thicker aluminum layer whose total absorption at energies 20–24 keV would be much higher than that of the used carbon window. A counterpart (5) and a heating system (6, 7) are the same as for the fluorescence cell. The transmission cell had a volume of 5.3 mL. Figure 2b shows the cell under operating conditions, including the environment and the beam path.

The total absorption of the transmission cell (from aluminum and Teflon) is 1.4 at Zr *K*-edge, while the absorption of water and organic liquids at this energy is already negligible. Thus, starting from Zr *K*-edge the sample can be optimized for high-quality transmission measurements. For the fluorescence cell at the same energy with the collection of Zr K_{α} emission, the total absorption is 1.2, which is also low enough for the measurement.

Photographs of cells, which were built according to the reported design, during the operation at the SAMBA beamline of the Soleil synchrotron (fluorescent cell) and STM beamline of the Kurchatov synchrotron radiation facility (transmission cell) are given in Figure 3a,b, respectively.

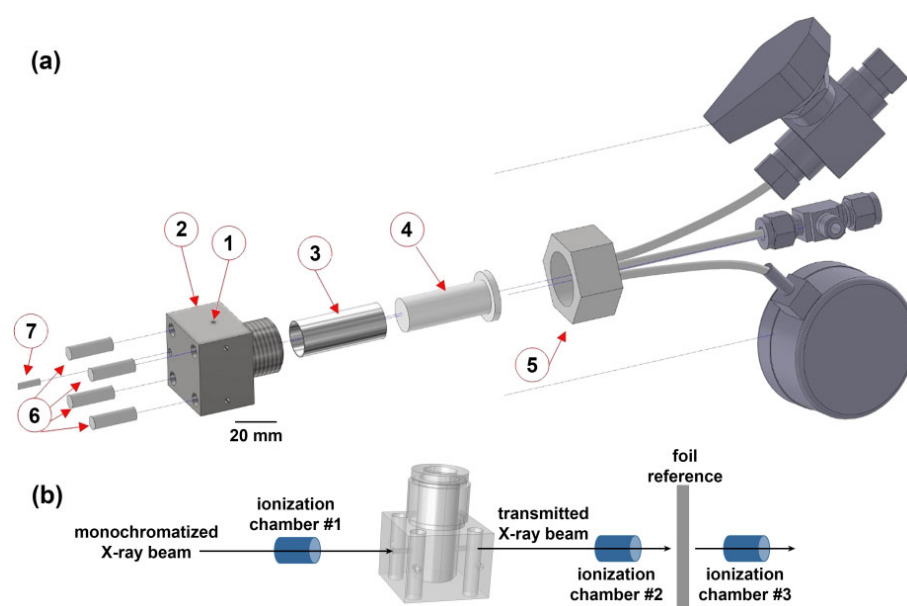


Figure 2. (a) Schematic view of the transmission cell. 1—hole, 2—cell body, 3—Al tube 0.5 mm thick, 4—Teflon reaction vessel, 5—sealing counterpart (screw, inlet, and outlet fittings, pressure gauge), 6—heating elements, 7—thermocouple. (b) Schematic view of the cell under operating conditions.

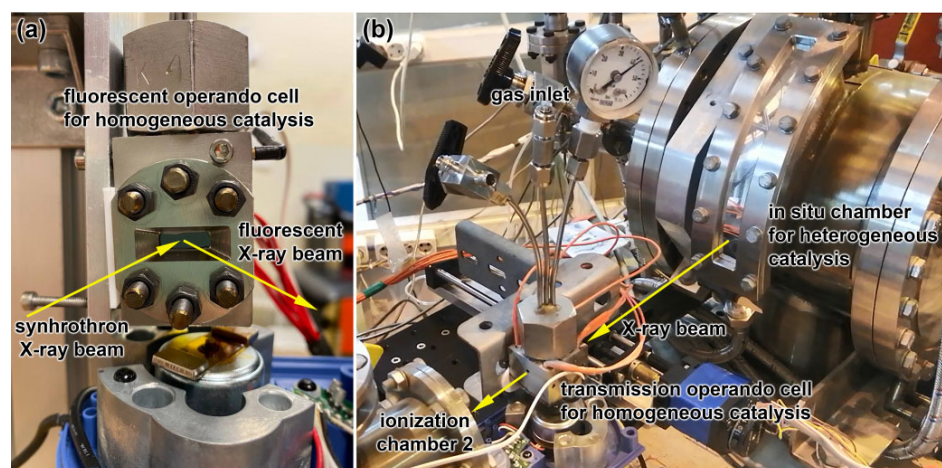


Figure 3. Photograph of the fluorescent (a) and transmission (b) cells during experiments at the synchrotron beamlines.

2.2. Cells Mechanical Stability

Before performing any real experiments in the designed cells, it was important to ensure that the devices could endure the required high pressures. Mechanical stability under 200 bar was checked using the “Solid Mechanics” module of COMSOL Multiphysics software (version 6.0, COMSOL AB, Stockholm, Sweden). Von Mises stress (σ) distributions for fluorescence and transmission cells are provided in Figure 4, parts a and b, respectively. For the first cell, the largest stress of 52 MPa was observed at the center of the window. The flexural and compressive strength of SIGRADUR® K material are 210 and 580 MPa, respectively, so the internal pressure of 200 bar can be considered safe. The maximum stress in the system of 100 MPa is achieved on the flange near the corners of the open part of the window and it is safely lower than the tensile strength for steel (500–700 MPa). For the transmission cell, the maximum stress on the aluminum tube was 135 MPa. The tube is made of aluminum 2024-T4, which has a tensile strength of about 450 MPa. So, both cells can be safely operated at 200 bar.

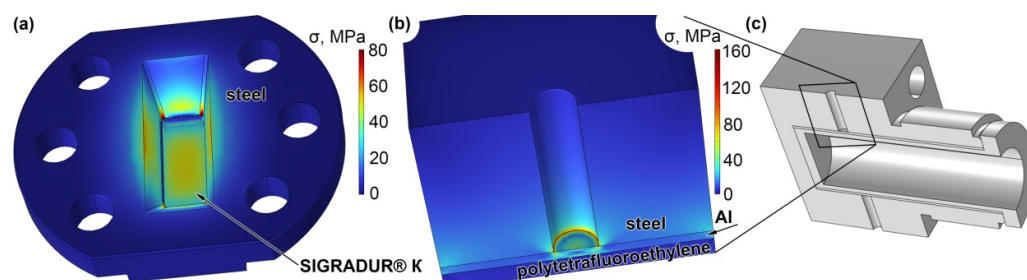


Figure 4. Von Mises stress (σ) distribution for fluorescence (a) and transmission (b) cells. Panel (c) shows the part of the transmission cell used for calculations.

2.3. Ru-Based Homogeneous Catalysis

The experimental test of the fluorescence cell was performed for Ru-based homogeneous catalyst for hydrodeoxygenation of sugar alcohols [30–33]. The concentration of Ru in the homogeneous catalytic system was too low to perform the data collection in a transmission geometry (the ratio between catalytic Ru species and buffer Br from the ionic liquid was Ru:Br = 1:35) therefore the spectra were collected in fluorescence mode. The system $\text{Bu}_4\text{PBr} + \text{RuBr}_3$ was studied under 5 bar of CO + 20 bar of H_2 . The presence of CO was necessary to form the active species for the hydrodeoxygenation reaction. X-ray absorption near-edge structure (XANES) spectra acquired at different temperatures are shown in Figure 5. At low temperatures, the ionic liquid was in a solid state and could not be distributed homogeneously inside the cell. Thus, the spectra above the melting point of ca. 100 °C have much better quality. The shape of XANES spectra for Ru species during the reaction differs significantly from the shape of the initial RuBr_3 precursor. At temperatures above 180 °C, the spectra of the sample are similar to that of the reference $\text{Ru}_2\text{Br}_4(\text{CO})_6$ [32]. Interestingly, it was this complex previously considered as an active catalyst in the reaction of hydrodeoxygenation of sugar alcohols [33]. Thus, in-situ measurements performed in the fluorescence cell allowed us to trace the formation of the Ru-based active complex via the interaction with CO ligands in a homogeneous catalytic system.

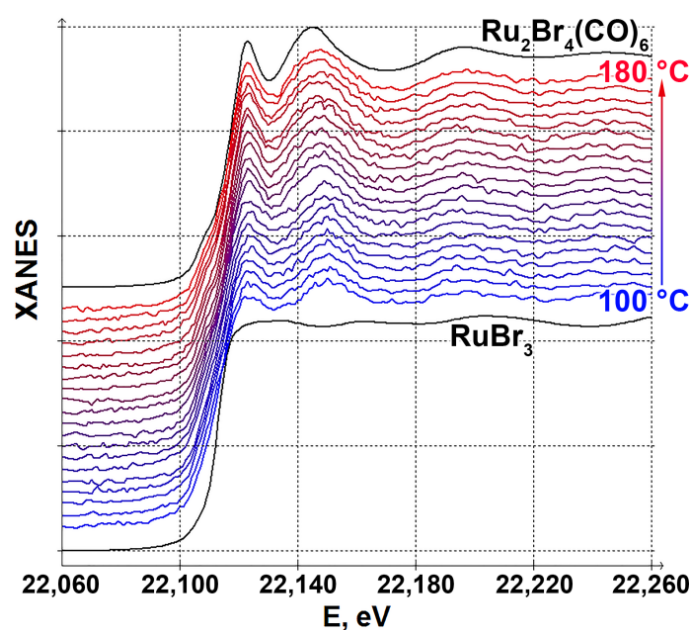


Figure 5. Ru K-edge XANES spectra acquired during the heating of the $\text{Bu}_4\text{PBr} + \text{RuBr}_3$ system under 5 bar of CO + 20 bar of H_2 . The top and bottom black lines are the reference spectra of $\text{Ru}_2\text{Br}_4(\text{CO})_6$ and RuBr_3 , respectively.

2.4. Rh-Based Homogeneous Catalysis

The Rh-based homogeneous catalytic system consisting of (Acetylacetonato) dicarbonylrhodium(I) [Rh(acac)(CO)₂] and triethylamine (Et₃N) in toluene solution was studied in the transmission cell. This catalyst is intended for the hydroformylation of olefins [34,35]. The reaction vessel was slowly heated to 80 °C under 100 bar of H₂ and CO (1:1) mixture. Figure 6a shows Rh *K*-edge XANES before and after heating. During the reaction, the near-edge region of the spectrum changes significantly without any shifting of the position of the absorption edge. We suggest that such a change of shape is caused by the substitution of one of the CO-groups in the initial complex by an Et₃N group. The extended X-ray absorption fine structure (EXAFS) of the same sample is shown in Figure 6b. It confirms that the initial single peak corresponding to the first shell of CO molecules split into two overlapped peaks: less coordinated CO and shell with larger interatomic distances, which might be attributed to the presence of the Et₃N group.

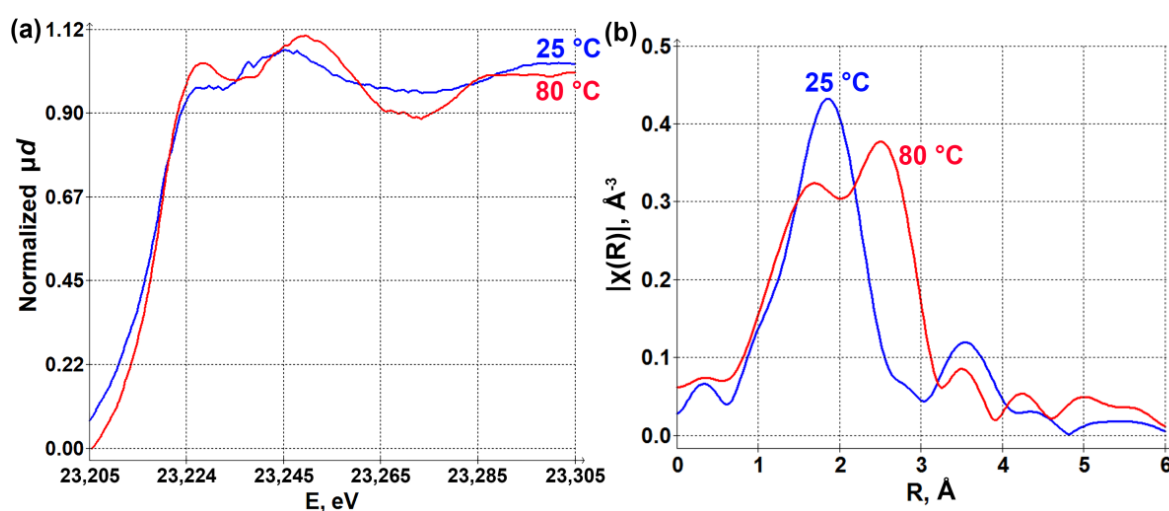


Figure 6. (a) Rh *K*-edge XANES spectra and (b) corresponding EXAFS data for Rh-catalyst at 25 °C and 80 °C.

Therefore, the performed study demonstrates that the local structure of rhodium sites is changing upon the reaction and the developed cell can be successfully used to track this evolution under the conditions relevant to industrial hydroformylation of Rh-based homogenous catalysts, which typically requires 50–150 bar of CO:H₂ (1:1–1:2).

2.5. Ru-Based Heterogeneous Catalysis

Figure 7a demonstrates Ru *K*-edge XANES of the Ru-based heterogeneous catalytic system intended for hydrogenation of bio-based hydrocarbons also studied in the transmission cell. In this case, the catalyst, initially present as a powder, was dispersed in water and sealed under 20 bar of H₂ with continuous stirring. The spectra were measured in transmission mode at temperatures from 25 to 200 °C. Upon the heating, we observed the shift of the absorption edge, which indicated the transition of ruthenium from the average oxidation state of Ru(IV) to Ru(II). The lower quality of spectra at room temperature is explained by the inhomogeneity of the reaction mixture. To overcome the issues of poor signal-to-noise ratio, which complicates the interpretation of individual spectra, we have applied principal component analysis (PCA) using PyFitIt code, to decompose the whole dataset into statistically relevant components [36,37]. Subsequent target matrix transformation allows one to convert the above components into physically meaningful spectra. It can be seen from Figure 7b, that the whole dataset shown in Figure 7a, is represented by the two independent states, corresponding to Ru(IV) and Ru(II) oxidation states according to the position of the edge. The concentration profiles of these two states are shown in

Figure 7c (the heating rate was about 2.2 deg/min until the system reached 200 °C at 80 min; afterward, the system was kept at 200 °C).

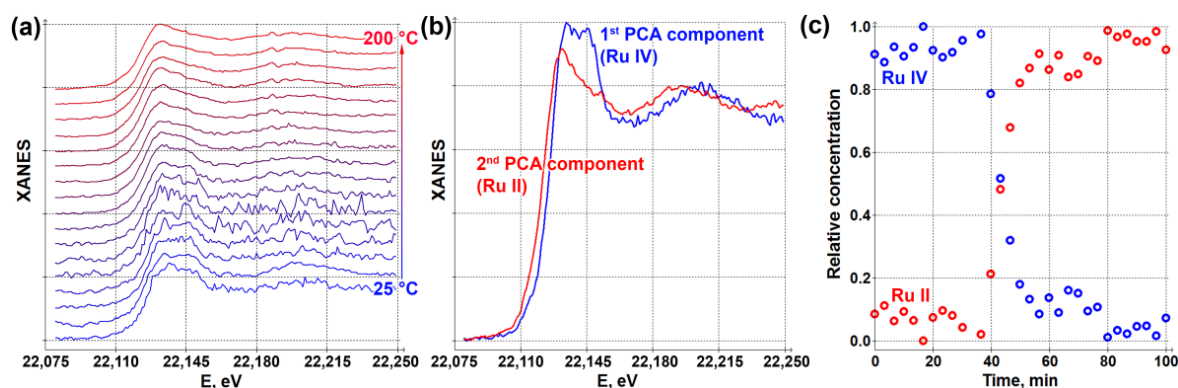


Figure 7. (a) Ru K-edge XANES spectra acquired during the heating of nanocatalyst. (b) The spectra of two components extracted by target matrix transformation of PCA components. (c) Concentration profiles corresponding to Ru(IV) and Ru(II) components.

The use of the transmission cell, therefore, allowed us to trace the evolution of the oxidation state of ruthenium in the liquid phase in the heterogeneous catalyst under high hydrogen pressures.

3. Materials and Methods

All chemicals for the present study were supplied by Sigma-Aldrich (St. Louis, MO, USA). The fluorescence was used for in situ measurements in fluorescence mode at the SAMBA beamline of the Soleil synchrotron (Paris, France). An X-ray beam was monochromatized using a Si (220) crystal. The absolute energy was initially calibrated by the spectrum of metallic ruthenium and was checked to be stable over the period of the experiment. Incident beam intensity was measured using an ionization chamber. The fluorescence signal was measured by a semiconductor detector (Vortex). The cell was applied to study Ru-based homogeneous catalytic systems [30,32,33]. Ruthenium bromide (RuBr_3) and $\text{Ru}_2\text{Br}_4(\text{CO})_6$ prepared similarly to the procedure described elsewhere [31] were used as a source of ruthenium. Ruthenium salts were dissolved in ionic liquids (tetrabutylphosphonium bromide Bu_4PBr or chloride Bu_4PCL) for the reaction of hydrodeoxygenation of sugar alcohols. We also included isopropyl alcohol as a model substrate and formaldehyde as a source of CO in the system. During the measurements, H_2 , CO, and Ar in different concentrations and a total pressure of 40 bar were supplied to the cell. The cell was heated from room temperature to 220 °C. A magnetic stirrer rotating at a frequency of 2 Hz was placed in the bottom of the cell.

The transmission cell was used for in situ measurements in transmission mode at the STM beamline of the Kurchatov synchrotron radiation facility (Institute of Synchrotron Research, Moscow, Russia). An X-ray beam was monochromatized using a Si (220) channel cut crystal. Variable energy step was applied in different regions of the absorption spectrum: 10 eV below the absorption edge, ~ 1 eV in the region around the edge, and 0.05 \AA^{-1} in the reciprocal space in the region of EXAFS. Higher harmonics were suppressed by detuning the monochromator. The X-ray beam intensity was measured by ionization chambers. The cell with a sample was placed between chamber #1 and chamber #2, and the reference sample of Rh foil was placed between chamber #2 and chamber #3 for energy calibration. The cell was used to study Rh-based homogeneous catalytic systems [38]. During the experiment, (Acetylacetonato)dicarbonylrhodium(I) $[\text{Rh}(\text{acac})(\text{CO})_2]$ was added to an excess solution of triethylamine (Et_3N) in toluene, and the system was slowly heated to 80 °C under the pressure of 100 bar of H_2 and CO mixture (1:1).

The same cell was then used for in situ measurements at the BM23 beamline of ESRF (Grenoble, France). A Si (311) crystal was used as a monochromator in continuous

scanning mode. Higher harmonics were suppressed by a rhodium mirror. The X-ray beam intensity was measured by ionization chambers. A ruthenium foil was a reference for energy calibration. The cell was used to study Ru-based heterogeneous catalytic reaction for the hydrogenation of organic crude materials [39]. A Ru-based catalytic sample was deposited on a porous aluminosilicate carrier. 200 mg of the sample was dispersed in 5 mL of water and placed into the cell under constant stirring. 20 bar of H₂ was then introduced into the cell, and the system was slowly heated up to 200 °C.

4. Conclusions

We have designed and manufactured two cells for in situ and, potentially, operando synchrotron XAS experiments optimized for the measurements in fluorescence and transmission modes. Both cells were successfully tested in operation at temperatures of up to 200 °C and under pressures of up to 200 bar, which was proved both by simulations and experimentally. Both cells were tested during in situ X-ray absorption experiments monitoring the evolution of homogeneous and heterogeneous catalytic systems in the liquid phase under reaction conditions. The experiment with the homogeneous low-concentrated Ru-based catalytic system in the high-Z ionic liquid buffer allowed us to trace the in-situ formation of the Ru₂Br₄(CO)₆ active complex. In the Rh-based homogeneous catalytic system, we applied transmission measurements due to the use of an X-ray transparent toluene solution and observed a substitution of one of the CO-groups in the initial complex by an Et₃N group. Finally, we monitored the evolution of the oxidation state from Ru(IV) to Ru(II) in the Ru-based heterogeneous catalytic system in water. Our results demonstrate the potential of the developed cells for studying the mechanisms of catalytic reactions under industrially relevant conditions.

Author Contributions: Conceptualization, P.A.P. and O.A.U.; methodology, A.L.B., E.R.N., D.N.G. and A.A.G.; software, P.V.S.; validation, E.R.N., A.A.G., O.A.U. and P.V.S.; formal analysis, D.N.G. and A.A.S.; investigation, V.R.Z., M.B.L., K.J., A.A.S., E.G.K., A.L.T. and E.F.; resources, A.I.D.; data curation, D.E.D.V. and V.V.S.; writing—original draft preparation, O.A.U., A.L.B., P.V.S. and A.I.D.; writing—review and editing, A.L.B. and P.V.S.; visualization, P.V.S.; supervision, A.V.S., A.Y.G. and D.E.D.V.; project administration, P.A.P. and A.Y.G.; funding acquisition, A.V.S. and A.Y.G. All authors have read and agreed to the published version of the manuscript.

Funding: This research was funded by the Ministry of Science and Higher Education of the Russian Federation, agreement No. 075-15-2021-1363.

Data Availability Statement: The data presented in this study are available in the article.

Acknowledgments: The authors acknowledge Kurchatov, Soleil, and ESRF synchrotron radiation facilities for the allocation of beamtimes and the staff of STM, ROCK, and BM23 beamlines for their kind support during the experiments.

Conflicts of Interest: The authors declare no conflict of interest. The funders had no role in the design of the study; in the collection, analyses, or interpretation of data; in the writing of the manuscript; or in the decision to publish the results.

References

1. Zhang, Y.; Fu, D.; Xu, X.; Sheng, Y.; Xu, J.; Han, Y. Application of operando spectroscopy on catalytic reactions. *Curr. Opin. Chem. Eng.* **2016**, *12*, 1–7. [[CrossRef](#)]
2. Bañares, M.A. Operando methodology: Combination of in situ spectroscopy and simultaneous activity measurements under catalytic reaction conditions. *Catal. Today* **2005**, *100*, 71–77. [[CrossRef](#)]
3. Urakawa, A. Trends and advances in Operando methodology. *Curr. Opin. Chem. Eng.* **2016**, *12*, 31–36. [[CrossRef](#)]
4. Lin, S.D.; Vannice, M.A. Hydrogenation of Aromatic Hydrocarbons over Supported Pt Catalysts. III. Reaction Models for Metal Surfaces and Acidic Sites on Oxide Supports. *J. Catal.* **1993**, *143*, 563–572. [[CrossRef](#)]
5. O'Brien, M.G.; Beale, A.M.; Jacques, S.D.M.; Di Michiel, M.; Weckhuysen, B.M. Closing the operando gap: The application of high energy photons for studying catalytic solids at work. *Appl. Catal. A-Gen.* **2011**, *391*, 468–476. [[CrossRef](#)]
6. Bordiga, S.; Groppo, E.; Agostini, G.; van Bokhoven, J.A.; Lamberti, C. Reactivity of Surface Species in Heterogeneous Catalysts Probed by In Situ X-ray Absorption Techniques. *Chem. Rev.* **2013**, *113*, 1736–1850. [[CrossRef](#)]

7. La Fontaine, C.; Barthe, L.; Rochet, A.; Briois, V. X-ray absorption spectroscopy and heterogeneous catalysis: Performances at the SOLEIL's SAMBA beamline. *Catal. Today* **2013**, *205*, 148–158. [[CrossRef](#)]
8. Briois, V.; La Fontaine, C.; Belin, S.; Barthe, L.; Moreno, T.; Pinty, V.; Carcy, A.; Girardot, R.; Fonda, E. ROCK: The new Quick-EXAFS beamline at SOLEIL. *J. Phys. Conf. Ser.* **2016**, *712*, 012149. [[CrossRef](#)]
9. Abdala, P.M.; Safonova, O.V.; Wiker, G.; van Beek, W.; Emerich, H.; van Bokhoven, J.A.; Sá, J.; Szlachetko, J.; Nachttegaal, M. Scientific Opportunities for Heterogeneous Catalysis Research at the SuperXAS and SNBL Beam Lines. *Chimia* **2012**, *66*, 699–705. [[CrossRef](#)]
10. Mondelli, C.; Ferri, D.; Grunwaldt, J.-D.; Krumeich, F.; Mangold, S.; Psaro, R.; Baiker, A. Combined liquid-phase ATR-IR and XAS study of the Bi-promotion in the aerobic oxidation of benzyl alcohol over Pd/Al₂O₃. *J. Catal.* **2007**, *252*, 77–87. [[CrossRef](#)]
11. O'Neill, B.J.; Miller, J.T.; Dietrich, P.J.; Sollberger, F.G.; Ribeiro, F.H.; Dumesic, J.A. Operando X-ray Absorption Spectroscopy Studies of Sintering for Supported Copper Catalysts during Liquid-phase Reaction. *ChemCatChem* **2014**, *6*, 2493–2496. [[CrossRef](#)]
12. Hoffman, A.S.; Debeve, L.M.; Bendjeriou-Sedjerari, A.; Ouldchikh, S.; Bare, S.R.; Basset, J.-M.; Gates, B.C. Transmission and fluorescence X-ray absorption spectroscopy cell/flow reactor for powder samples under vacuum or in reactive atmospheres. *Rev. Sci. Instrum.* **2016**, *87*, 073108. [[CrossRef](#)]
13. Hansen, B.R.S.; Møller, K.T.; Paskevicius, M.; Dippel, A.-C.; Walter, P.; Webb, C.J.; Pistidda, C.; Bergemann, N.; Dornheim, M.; Klassen, T.; et al. In situ X-ray diffraction environments for high-pressure reactions. *J. Appl. Cryst.* **2015**, *48*, 1234–1241. [[CrossRef](#)]
14. Rai, D.K.; Gillilan, R.E.; Huang, Q.; Miller, R.; Ting, E.; Lazarev, A.; Tate, M.W.; Gruner, S.M. High-pressure small-angle X-ray scattering cell for biological solutions and soft materials. *J. Appl. Cryst.* **2021**, *54*, 111–122. [[CrossRef](#)]
15. Meira, D.M.; Monte, M.; Fernández-García, M.; Meunier, F.; Mathon, O.; Pascarelli, S.; Agostini, G. A flexible cell for in situ combined XAS–DRIFTS–MS experiments. *J. Synchrotron Rad.* **2019**, *26*, 801–810. [[CrossRef](#)]
16. Ahmad, M.I.; Van Campen, D.G.; Fields, J.D.; Yu, J.; Pool, V.L.; Parilla, P.A.; Ginley, D.S.; Van Hest, M.F.A.M.; Toney, M.F. Rapid thermal processing chamber for in-situ x-ray diffraction. *Rev. Sci. Instrum.* **2015**, *86*, 013902. [[CrossRef](#)]
17. Bertram, F.; Deiter, C.; Pflaum, K.; Seeck, O.H. A compact high vacuum heating chamber for in-situ x-ray scattering studies. *Rev. Sci. Instrum.* **2012**, *83*, 083904. [[CrossRef](#)]
18. Xto, J.; Wetter, R.; Borca, C.N.; Frieh, C.; van Bokhoven, J.A.; Huthwelker, T. Droplet-based in situ X-ray absorption spectroscopy cell for studying crystallization processes at the tender X-ray energy range. *RSC Adv.* **2019**, *9*, 34004–34010. [[CrossRef](#)]
19. Bauer, M.; Heusel, G.; Mangold, S.; Bertagnolli, H. Spectroscopic set-up for simultaneous UV-Vis/(Q)EXAFS in situ and in operando studies of homogeneous reactions under laboratory conditions. *J. Synchrotron Rad.* **2010**, *17*, 273–279. [[CrossRef](#)]
20. Liu, H.; Allan, P.K.; Borkiewicz, O.J.; Kurtz, C.; Grey, C.P.; Chapman, K.W.; Chupas, P.J. A radially accessible tubular in situ X-ray cell for spatially resolved operando scattering and spectroscopic studies of electrochemical energy storage devices. *J. Appl. Cryst.* **2016**, *49*, 1665–1673. [[CrossRef](#)]
21. Borkiewicz, O.J.; Shyam, B.; Wiaderek, K.M.; Kurtz, C.; Chupas, P.J.; Chapman, K.W. The AMPIX electrochemical cell: A versatile apparatus for in situ X-ray scattering and spectroscopic measurements. *J. Appl. Cryst.* **2012**, *45*, 1261–1269. [[CrossRef](#)]
22. Bravo-Suárez, J.J.; Srinivasan, P.D. Design characteristics of in situ and operando ultraviolet-visible and vibrational spectroscopic reaction cells for heterogeneous catalysis. *Catal. Rev.* **2017**, *59*, 295–445. [[CrossRef](#)]
23. Nguyen, L.; Tao, F. Development of a reaction cell for in-situ/operando studies of surface of a catalyst under a reaction condition and during catalysis. *Rev. Sci. Instrum.* **2016**, *87*, 064101. [[CrossRef](#)] [[PubMed](#)]
24. Kristiansen, P.T.; Rocha, T.C.R.; Knop-Gericke, A.; Guo, J.H.; Duda, L.C. Reaction cell for in situ soft x-ray absorption spectroscopy and resonant inelastic x-ray scattering measurements of heterogeneous catalysis up to 1 atm and 250 °C. *Rev. Sci. Instrum.* **2013**, *84*, 113107. [[CrossRef](#)]
25. Lurio, L.; Mulders, N.; Paetkau, M.; Jemian, P.R.; Narayanan, S.; Sandy, A. Windows for small-angle X-ray scattering cryostats. *J. Synchrotron Rad.* **2007**, *14*, 527–531. [[CrossRef](#)]
26. Liu, L.; He, P.; Xia, Y.; Song, H.; Chang, L.-Y.; Chen, J.-L.; Pao, C.-W. X-ray absorption fine structure measurements on Ru-Zn/ZSM-5 during heterogeneous catalysis using an in situ spectroscopic cell. *Electron. Struct.* **2020**, *2*, 034002. [[CrossRef](#)]
27. Grabow, K.; Bentrup, U. Homogeneous Catalytic Processes Monitored by Combined in Situ ATR-IR, UV-Vis, and Raman Spectroscopy. *ACS Catal.* **2014**, *4*, 2153–2164. [[CrossRef](#)]
28. Iggo, J.A.; Shirley, D.; Tong, N.C. High pressure NMR flow cell for the in situ study of homogeneous catalysis. *New J. Chem.* **1998**, *22*, 1043–1045. [[CrossRef](#)]
29. Schneider, M.S.; Grunwaldt, J.-D.; Bürgi, T.; Baiker, A. High pressure view-cell for simultaneous in situ infrared spectroscopy and phase behavior monitoring of multiphase chemical reactions. *Rev. Sci. Instrum.* **2003**, *74*, 4121. [[CrossRef](#)]
30. Janssens, K.; Bugaev, A.L.; Kozyr, E.G.; Lemmens, V.; Guda, A.A.; Usoltsev, O.A.; Smolders, S.; Soldatov, A.V.; De Vos, D.E. Evolution of the active species of homogeneous Ru hydrodeoxygenation catalysts in ionic liquids. *Chem. Sci.* **2022**, *13*, 10163–10584. [[CrossRef](#)]
31. Janssens, K.; Stalpaert, M.; Henrion, M.; De Vos, D.E. From crude industrial waste glycerol to biopropene via Ru-mediated hydrodeoxygenation in ionic liquids. *Chem. Commun.* **2021**, *57*, 6324–6327. [[CrossRef](#)]
32. Kozyr, E.G.; Bugaev, A.L.; Guda, S.A.; Guda, A.A.; Lomachenko, K.A.; Janssens, K.; Smolders, S.; de Vos, D.; Soldatov, A.V. Speciation of Ru Molecular Complexes in a Homogeneous Catalytic System: Fingerprint XANES Analysis Guided by Machine Learning. *J. Phys. Chem. C* **2021**, *125*, 27844–27852. [[CrossRef](#)]

33. Stalpaert, M.; Janssens, K.; Marquez, C.; Henrion, M.; Bugaev, A.L.; Soldatov, A.V.; De Vos, D. Olefins from Biobased Sugar Alcohols via Selective, Ru-Mediated Reaction in Catalytic Phosphonium Ionic Liquids. *ACS Catal.* **2020**, *10*, 9401–9409. [[CrossRef](#)]
34. Bruss, A.J.; Gelesky, M.A.; Machado, G.; Dupont, J. Rh(0) nanoparticles as catalyst precursors for the solventless hydroformylation of olefins. *J. Mol. Catal.* **2006**, *252*, 212–218. [[CrossRef](#)]
35. Chikkali, S.H.; Bellini, R.; de Bruin, B.; van der Vlugt, J.I.; Reek, J.N.H. Highly Selective Asymmetric Rh-Catalyzed Hydroformylation of Heterocyclic Olefins. *J. Am. Chem. Soc.* **2012**, *134*, 6607–6616. [[CrossRef](#)]
36. Martini, A.; Guda, S.A.; Guda, A.A.; Smolentsev, G.; Algasov, A.; Usoltsev, O.; Soldatov, M.A.; Bugaev, A.; Rusalev, Y.; Lamberti, C.; et al. PyFitit: The software for quantitative analysis of XANES spectra using machine-learning algorithms. *Comput. Phys. Commun.* **2020**, *250*, 107064. [[CrossRef](#)]
37. Usoltsev, O.A.; Bugaev, A.L.; Guda, A.A.; Guda, S.A.; Soldatov, A.V. How much structural information could be extracted from XANES spectra for palladium hydride and carbide nanoparticles. *J. Phys. Chem. C* **2022**, *126*, 4921–4928. [[CrossRef](#)]
38. Nenasheva, M.; Gorbunov, D.; Karasaeva, M.; Maximov, A.; Karakhanov, E. Non-phosphorus recyclable Rh/triethanolamine catalytic system for tandem hydroformylation/hydrogenation and hydroaminomethylation of olefins under biphasic conditions. *Mol. Catal.* **2021**, *516*, 112010. [[CrossRef](#)]
39. Panagiotopoulou, P.; Vlachos, D.G. Liquid phase catalytic transfer hydrogenation of furfural over a Ru/C catalyst. *Appl. Catal. A-Gen.* **2014**, *480*, 17–24. [[CrossRef](#)]